Evaluation of segmentation methods for RGB colour image-based detection of Fusarium infection in corn grains using support vector machine (SVM) and pre-trained convolution neural network (CNN)

T.S. Rathna Priya and Annamalai Manickavasagan*

[2]*School of Engineering, University of Guelph, Guelph, Ontario, Canada, N1G 2W1 Canada*

**Corresponding Author: mannamal@uoguelph.ca*

ABSTRACT

This study evaluated six segmentation methods (clustering, flood-fill, graph-cut, colour-thresholding, watershed, and Otsu's-thresholding) for segmentation accuracy and classification accuracy in discriminating *Fusarium* infected corn grains using RGB colour images. The segmentation accuracy was calculated using Jaccard similarity index and Dice coefficient in comparison with the gold standard (manual segmentation method). Flood-fill and graph-cut methods showed the highest segmentation accuracy of 77% and 87% for Jaccard and Dice evaluation metrics, respectively. Pre-trained convolution neural network (CNN) and support vector machine (SVM) were used to evaluate the effect of segmentation methods on classification accuracy using segmented images and extracted features from the segmented images, respectively. The SVM based two-class model to discriminate healthy and *Fusarium* infected corn grains yielded the classification accuracy of 84%, 79%, 78%, 74%, 69% and 65% for graph-cut, watershed, clustering, flood-fill, colour-thresholding, and Otsu's-thresholding, respectively. In pretrained CNN model, the classification accuracies were 93%, 88%, 87%, 84%, 61% and 59% for flood-fill, graph-cut, colour-thresholding, clustering, watershed, and Otsu's-thresholding, respectively. Jaccard and Dice evaluation metrics showed the highest correlation with the pretrained CNN classification accuracies with R^2 values of 0.9693 and 0.9727, respectively. The correlation with SVM classification accuracies were R^2–0.505 for Jaccard and R^2–0.5151 for Dice evaluation metrics.

KEYWORDS

corn, imaging, segmentation, classification, algorithm, accuracy, *Fusarium*

RÉSUMÉ

Cette étude a permis d'évaluer six méthodes de segmentation (groupage [clustering], élimination des petites zones isolées [flood fill], segmentation graphique [graph-cut], seuillage de couleur [colour-thresholding], ligne de partage des eaux [watershed], et la méthode d'Otsu [Otsu's-thresholding] utilisées pour déterminer la précision de segmentation et la précision de classification pour discerner les grains de maïs infectés par le *Fusarium* en utilisant des images couleur RVB. La précision de la segmentation a été calculée à l'aide de l'indice de similarité de Jaccard et du coefficient de Dice en comparaison avec l'étalon de référence (méthode de segmentation manuelle). Les méthodes Flood-fill et graph-cut ont montré la plus grande précision de segmentation de 77 % et 87 % pour les paramètres d'évaluation de Jaccard et Dice, respectivement. Un réseau de neurones convolutif [CNN] préentraîné et une machine à vecteur de support (SVM) ont été utilisés pour évaluer l'effet des méthodes de segmentation sur la précision de la classification en utilisant les images segmentées et les caractéristiques extraites des images segmentées, respectivement. Le modèle à deux classes fondé sur le SVM pour distinguer les grains de maïs sains des grains infectés par le *Fusarium* a donné une précision de classification de 84 %, 79 %, 78 %, 74 %, 69 % et 65 % pour les méthodes graph-cut, watershed, clustering, flood-fill, colour-thresholding et Otsu's-thresholding, respectivement. Dans le modèle CNN préentraîné, les précisions de classification étaient de 93 %, 88 %, 87 %, 84 %, 61 % et 59 % pour les méthodes flood-fill, graph-cut, colour-thresholding, clustering, watershed, et Otsu's-thresholding, respectivement. Les paramètres d'évaluation de Jaccard et de Dice ont montré la plus forte corrélation avec les précisions de classification CNN préentrainées et avec des valeurs R^2 de 0,9693 et 0,9727, respectivement. La corrélation avec les précisions de classification de la SVM était d'un R^2 de -0.505 pour les paramètres d'évaluation de Jaccard et d'un R^2 de -0.5151 pour ceux de Dice.

MOTS CLÉS

maïs, imagerie, segmentation, classification, algorithme, précision, *Fusarium*

CITATION

Rathna Priya, T.S. and A. Manickavasagan. 2022. **Evaluation of segmentation methods for RGB colour image-based detection of Fusarium infection in corn grains using support vector machine (SVM) and pre-trained convolution neural network (CNN).** Canadian Biosystems Engineering/Le génie des biosystèmes au Canada 64: 7.9-7.20. https://doi.org/10.7451/CBE.2022.64.7.9

INTRODUCTION

Grain corn is the world's highest-produced cereal crop, with production at 1.09 billion metric tonnes (Statistics Canada 2020; Saldivar and Carrillo 2019). Corn grown in fields possess high moisture content and warm temperature (25 - 28°C) which are favourable for the growth of several fungal species. The starch present in the grains serves as an excellent medium for their fast growth and development. The most common fungal species grown in corn grains are *Fusarium graminearum, Fusarium culmorum and, Fusarium vertcilloides* (Fiore et al. 2010; Kushiro 2008). These toxigenic fungi upon further favourable conditions produces secondary metabolites called mycotoxins, which remain stable in the grain for a long time.

One common mycotoxin produced by these *Fusarium* species is called deoxynivalenol (DON), which belongs to a group called trichothecenes. Trichothecene mycotoxins are a group of over 148 structurally related compounds produced by the *Fusarium* species of which DON is the most common mycotoxin. Several acute poisoning incidences have been linked to the consumption of *Fusarium* infected, in particular, DON contaminated foods (Pestka 2010).

Although many techniques like thin layer chromatography (TLC), high pressure liquid chromatography (HPLC) and gas chromatography (GC) exist for the detection of these fungal mycotoxin, these are not applicable for online evaluation in real time applications (Ran et al. 2013). At present, random sampling is performed by picking probe samples from each truck and a subsample is taken from the probe samples for determining fungal infected grains or presence of DON. This approach may not provide accurate information about the presence of *Fusarium* infected corn grains in the truck. The accurate identification of healthy and infected grains from a whole batch of grains is nearly impossible by means of visual inspection (Agelet et al. 2012). Furthermore, to our knowledge, currently there is no technique available to identify and remove *Fusarium* infected corn grains during handling or storage or processing. The existing analytical techniques are very lengthy, time consuming and highly expensive.

Thus, image-based non-destructive methods could offer a solution for the efficient identification and removal of *Fusarium* infected corn grains from the supply chain. Although there are many studies on the different imaging techniques to detect the fungal infections, especially aflatoxin contamination in corn, there are very limited studies to detect *Fusarium* infection in corn (Priya and Manickavasagan 2021).

In any image-based classification method, image segmentation is the process of separating or dividing a digital image into different segments including the regions of interest (foreground) and background pixels. This process is crucial as it converts the image into a more useful data that would be easier to analyze. Image segmentation is the foremost step in image analysis and image classification. Segmentation assigns a label to every pixel in an image and pixels with the same label share similar characteristics or properties which will be extracted as features and utilized for classification model development. Poor segmentation will lose important feature information from the region of interest (ROI) or include wrong information from the background, either case the collected feature is not true information and ends up in wrong classification. There are several methods available for segmentation including histogram thresholding, colour thresholding, Otsu's thresholding, clustering, region growing, mean shift, graph cut, local graph cut, watershed, edge detection based, object based, partial differential equation-based methods. However, there is no standard or accurate method that can be applied to all images. Based on the application and type of images, the segmentation method should be selected accordingly (Pal and Pal 1993). In most of the imaging-based agriculture and food applications, random segmentation methods are used, and various classification techniques are evaluated. When inaccurate features are extracted from the ROI through wrong segmentation method, the classification accuracies will be seriously affected.

The objective of this study was to evaluate the accuracy of six segmentation methods for touching and non-touching corn grains in RGB colour images and determine their impact on the classification accuracy to detect *Fusarium* infection.

METHODOLOGY

Sample collection

Healthy and *Fusarium* infected corn grains harvested in the year 2017 were obtained from the Ontario Ministry of Agriculture, Food and Rural Affairs (OMAFRA). The samples were precleaned manually to remove the husk, broken kernels and stored at -20 °C until image acquisition.

Image acquisition

The grain images were captured using single lens reflex digital camera Nikon D7500 with 5568×3712 image area (pixels) and complementary metal oxide semiconductor (CMOS) sensor. A black background was used for capturing the images to minimize the reflection.

Touching and non-touching grains The RGB images of corn grains from both healthy set and *Fusarium* infected set were captured. The images had been labelled and were divided into two groups.

In the first group, the corn grains were arranged in a designed line pattern where all grains were separated from each other and had non-touching grains. Each image contained around 20 corn grains. For every 20 corn grains, the germ side and the endosperm side were captured separately. This was done to observe if there is any variation in the efficiency of the segmentation algorithms in detecting the germ portion of the corn kernels. The germ portion of the kernels slightly vary in colour (white to creamy white) when compared with the endosperm portion (bright to light yellow). The healthy kernels set comprised of 200 images

(100 with germ side, 100 with endosperm side). Similarly, the infected kernels set comprised of 200 images (100 with germ side and 100 with endosperm side). In the second group, the corn grains were randomly distributed without any specific pattern and had monolayer touching corn grains. Each image had around 100 corn grains. The endosperm and the germ side of the grains were captured separately. The images were taken for both the healthy and *Fusarium* infected corn grains. The healthy set and *Fusarium* infected set each comprised of 100 images, 50 with germ side and 50 with endosperm side, respectively. Overall, the healthy kernel set (group 1 and 2) had 300 images and infected kernel set (group 1 and 2) had 300 images.

Segmentation methods

The most common segmentation methods that have been used for wide range of image based food applications were chosen for this study. The images in the datasets were subjected to each of the segmentation methods and the segmented binary image and masked image were separately stored for evaluating similarity metrics.

Gold standard segmentation Each image from the dataset (total 600 images) had been segmented by manual segmentation and was considered as the gold standard method. The boundary separating the background and foreground had been drawn manually for individual corn grains by encircling the regions of interest (ROI) to obtain a binary mask. The binary image was then applied on to the original image to get the segmented or masked image.

Clustering segmentation Clustering is an unsupervised image segmentation technique. Based on the values initialized to the pixels, the algorithm classifies and groups the pixels into numerous clusters. The number of clusters can either be defined or undefined based on the user initialization. The algorithm trains itself using the existing data and identifies the clusters as the foreground, thus segmenting the objects of interest (Dhanachandra and Chanu 2017). A random number of clusters were initially chosen and each datapoint or pixel in the image was assigned to one of the clusters such that the distance between the pixel and cluster centre is minimum. The cluster centres were again recomputed at the end by taking the average of all the pixels in the cluster. This step was repeated until convergence was attained.

Flood Fill based object segmentation This technique, also called the seed fill algorithm determines the regions in an image connected to an initialized node in a multi-dimensional array. The algorithm identifies the connected nodes belonging to the ROIs and by the given target node and changes them to the replacement node till the boundary is reached. The flood-fill operation was performed based on the Euclidean distance from the start node and the tolerance was optimized for the healthy and *Fusarium* infected grains separately (Lee and Kang 2010).

Graph cut segmentation This algorithm considers each image as a graph with terminals and links, thereby achieving faster segmentation. Every pixel is treated as node connected through weighted links. The probability of relations between similar nodes (intensity based) determine the weights of the links. The algorithm uses a max-flow min- cut method to determine the minimum cut with the smallest cost in polynomial time. Then the cut is made along the weaker links to split the pixels along the two terminals: the source and the sink, yielding the segmented image (Veksler 2008).

Colour thresholding This algorithm was used to segment the ROIs by thresholding individual colour channels based on different colour spaces. A binary segmentation mask was created for each colour image. The colour channels were optimized in the RGB colour space by windowing the intensities of colour channel and based on the three thresholds for each colour channel, the images were segmented (Kulkarni 2010).

Watershed segmentation Watershed algorithm treats each image as a topographical surface with peaks and troughs. The peaks and troughs correspond to the intensities of the grey level of each pixel in the image. The regional minima are then identified, and a flooding process is simulated to determine the hierarchical queue. At the end, each pixel is assigned to a labelled region which depicts the segmented image (Bieniek and Moga 2000; Longzhe 2011). The colour image was read and converted into grayscale. The gradient magnitude was computed for the image as a segmentation function. The foreground and background of the object was marked, and the watershed transformation of the segmentation function was then computed. Watershed algorithm for image segmentation is one of the oldest methods that finds application as a powerful tool for segmenting objects and is advantageous mainly because it provides closed contours (Belaid and Mourou 2009).

Otsu's thresholding Otsu's method is an automatic segmentation technique that identifies the optimal intensity threshold level after accounting the intensities of every pixel in an image. The threshold value distinguishes and assigns the pixels to either the foreground or background. The threshold value was determined by minimizing the intensity variance in the two classes after assigning each pixel. This technique is a discrete analog of Fisher's Discriminant Analysis. The algorithm determines the threshold level such that the intensity variation between the two groups is maximum and that within each group is kept minimum (Sha et al. 2016). An automatic thresholding technique for segmenting the background objects from the corn germplasm was developed by modifying the Otsu's algorithm using a probability theory. This thresholding method was found to perform better than the Otsu's algorithm with high accuracy and also eliminated the misclassification that occurred in Otsu's algorithm (Panigrahi et al.1995).

Segmentation accuracy

Though all the segmentation methods seemed to segment the grains, quantitative results are necessary to accurately identify the accuracy of each segmentation method. Therefore, segmentation evaluation metrics such as Jaccard

similarity index and Dice similarity coefficient were used to evaluate the accuracy of each segmentation method (Senthilkumaran and Vaithegi 2016; Skourt et al. 2018). The segmented mask from each method was applied on the original image to get the regions of interest. The segmentation accuracy was determined by comparing the segmented image with that of the gold standard.

Jaccard similarity index Jaccard index evaluates the similarity between the segmented image and the gold standard and returns an index which is the ratio of similar pixels to the total number of pixels in the two images (McAllister 2018). If the gold standard is considered as the ground truth (G) and the segmentation result as S, then Jaccard index can be given as

$$E = \frac{A(G \cap S)}{A(G \cup S)}, \quad (1)$$

where A(.) corresponds to operation of counting amount, numerator corresponds to the total number of matching pixels and denominator corresponds to the total number of matching and mismatching pixels.

Dice coefficient Dice coefficient is similar to Jaccard index except that it considers the similarity in pixels in both the images individually and compares it with the total number of pixels in the images (Skourt et al. 2018). If the gold standard is considered as the ground truth (G) and the segmentation result as S, then Dice coefficient is given as

$$E = \frac{2 * A(G \cap S)}{A(G \cup S)}, \quad (2)$$

where numerator corresponds to the total number of overlapping or matching pixels in both the images and the denominator corresponds to the total number of pixels in both the images. Jaccard metrics penalises every instance of mismatched pixels and depicts the worst-case scenario whereas Dice metrics returns the average performance of the algorithm. Both the metrics were applied to each of the segmentation algorithms for every image.

Classification models

Support vector machine model The segmented images of each of the methods were processed further for feature extraction and classification in MATLAB R2019b software. A total of 9 colour features and 13 geometric features were extracted from each segmented image (Table 1) and used to develop a classification model based on support vector machine (SVM) multiclass classifier using the image category classifier. The model was first trained with the images in the training set and the accuracy was determined by plotting a confusion matrix between the true and predicted classes. Then, the images in the validation set were evaluated with the developed model and the accuracy was determined by plotting a confusion matrix. The mean accuracy of the classification model in discriminating between the healthy and *Fusarium* infected corn grains was finally determined.

Pre-trained CNN model In recent years, research has been focused on extracting the deep features from pretrained convolutional neural networks (CNNs) to train machine learning classification models. These trained classifiers are

Table 1. Features extracted from the images of healthy and Fusarium infected corn grains.

Features		Description
Colour Features	Mean R	Measure of average red intensity (0 to 255) in RGB colour space
	Mean G	Measure of average green intensity (0 to 255) in RGB colour space
	Mean B	Measure of average blue intensity (0 to 255) in RGB colour space
	Mean H	Measure of average hue (0 to 360°) in HSI colour space
	Mean S	Measure of average saturation (0 to 1) in HSI colour space
	Mean I	Measure of average intensity (0 to 1) in HSI colour space
	Mean L*	Measure of average lightness (0 to 100) in L*a*b* colour space
	Mean a*	Measure of average red and green pixels (-128 – 127) in L*a*b* colour space
	Mean b*	Measure of average blue and yellow pixels (-128 – 127) in L*a*b* colour space
Geometric features	Centroid	X and y coordinates of the center of mass
	Major Axis	Measure of the length of major axis of the ellipse, in pixels
	Minor Axis	Measure of the length of minor axis of the ellipse, in pixels
	Eccentricity	Ratio of the distance between foci of the ellipse and major axis length
	Filled Area	Measure of number of on pixels in filled image
	Area	Measure of actual number of pixels in the region
	Perimeter	Measure of the distance around the boundary of the region
	Convex area	Measure of the number of pixels in convex image
	Extent	Measure of ratio of pixels to pixels in the smallest box containing the region
	Max Feret	Max distance between any 2 boundary points on the vertices of convex hull that
	Min Feret	Min distance between any 2 boundary points on the vertices of convex hull that encloses
	EquivDiameter	Measure of the diameter of a circle with the same area as the region
	Solidity	Proportion of the pixels in the convex area that are also present in the region

All geometric features are pixels, returned as a scalar.

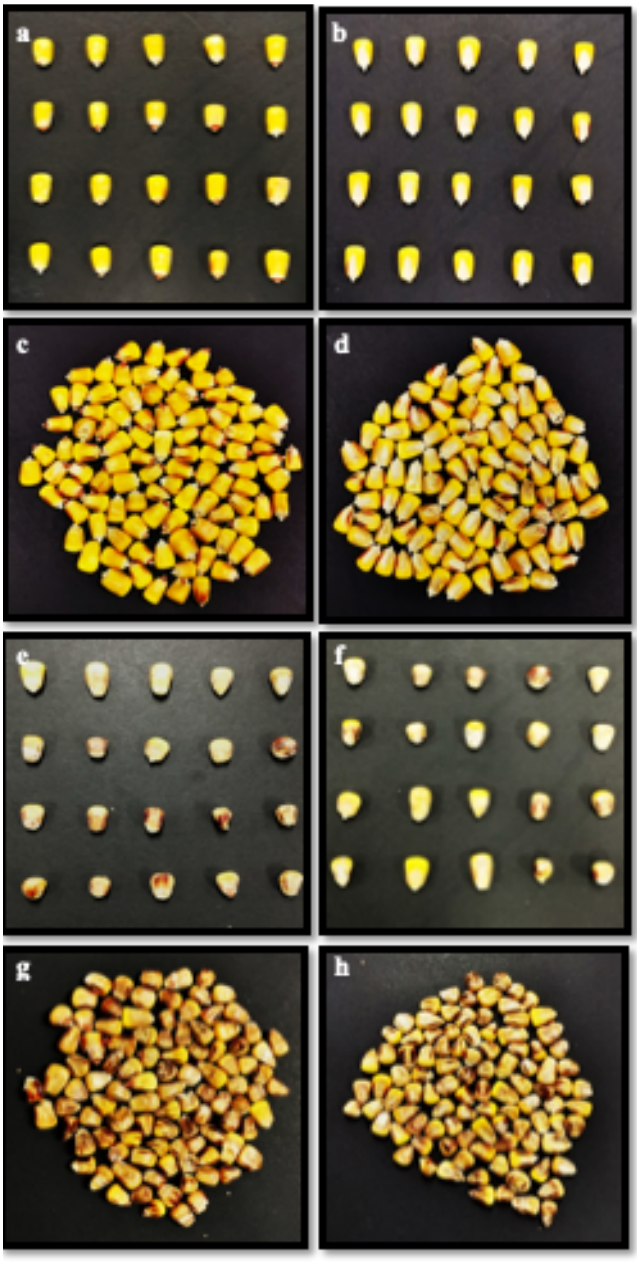

Fig 1. Sample images of non-touching and touching corn grains (a) Healthy - non-touching - endosperm side (b) Healthy - non touching - germ side (c) Healthy – touching - endosperm side (d) Healthy – touching - germ side (e) Fusarium infected - non touching - endosperm side (f) Fusarium infected - non touching - germ side (g) Fusarium infected – touching - endosperm side (h) Fusarium infected - touching - germ side.

further used for image classification. The established pretrained CNN architectures include AlexNet, GoogleNet, VGG-16 etc., which are opted for deep feature extraction for image classification (Yuheng and Hao 2017). Teachable Machine by Google, a web-based tool that is utilized for quickly training a deep learning image classification model

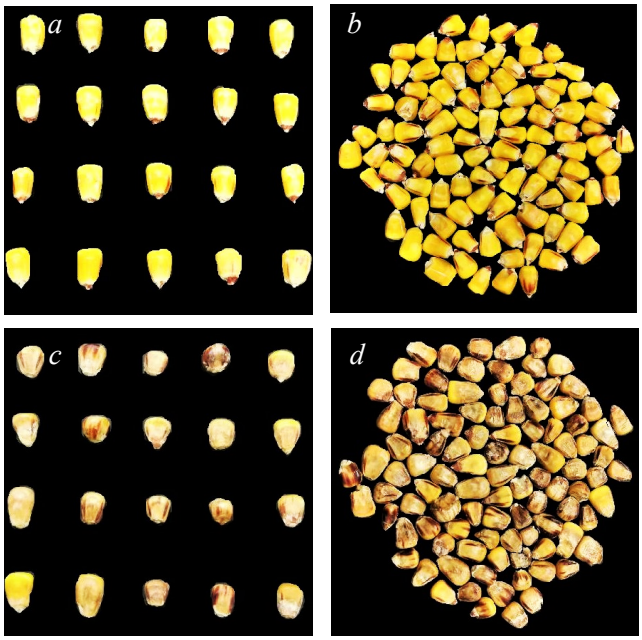

Fig 2. Segmented images from the gold standard method (a) Healthy - non touching (b) Healthy - touching (c) Fusarium infected - non touching (d) Fusarium infected - touching.

was used in this study. This model is based on TensorFlow and uses a technique called transfer learning where the model would be pre-trained on a large dataset and the convolution layers are trained for accurate feature extraction. Only few layers like epoch and learning rate needs to be optimized as per specific model requirements.

The classification efficiency of individual segmentation method was determined with the segmented images using this pre-trained model (80:20 training:test). For comparison, the classification accuracy of original images (without segmentation) was also determined in the same approach.

Statistical analysis

The effect of segmentation method, grain type and grain arrangement on segmentation accuracy was analyzed by three-way analysis of variance (ANOVA) method using R studio software (version 3.6.1). The post hoc Tukey HSD test with a 0.05 level of significance was performed to analyze if the independent variables had significant differences on the segmentation accuracy. The differences within the levels under each segmentation evaluation metrics were tested using the least significant difference (LSD) method of comparison of means.

RESULTS AND DISCUSSION

Evaluation of segmentation methods

The sample images from healthy and *Fusarium* infected corn grain groups are shown in Fig 1.

Gold standard segmentation. Since the segmentation was manual, (Fig 2), the regions of interest inside each corn grain were captured for healthy as well as *Fusarium*

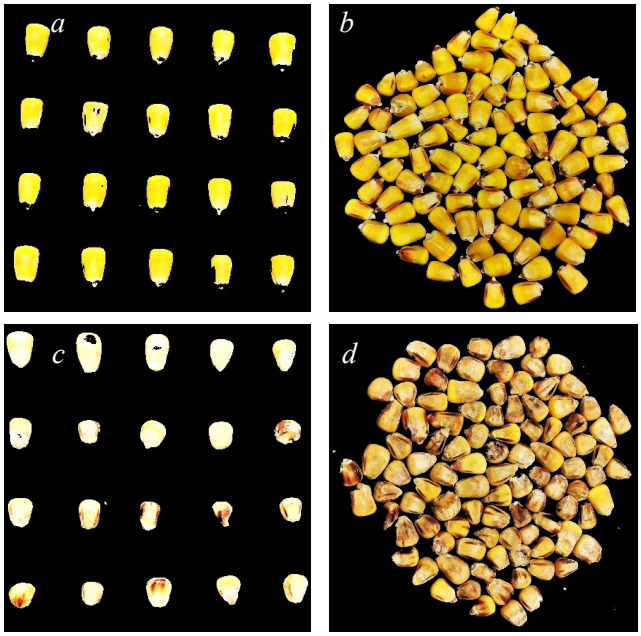

Fig 3. Segmented images from clustering method (a) Healthy - non touching (b) Healthy - touching (c) Fusarium infected - non touching (d) Fusarium infected – touching.

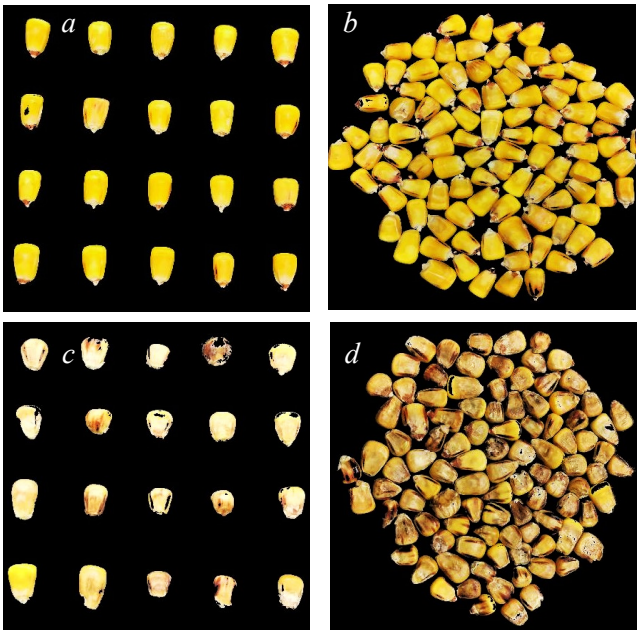

Fig. 4. Segmented images from the flood fill method (a) Healthy - non touching (b) Healthy - touching (c) Fusarium infected - non touching (d) Fusarium infected - touching.

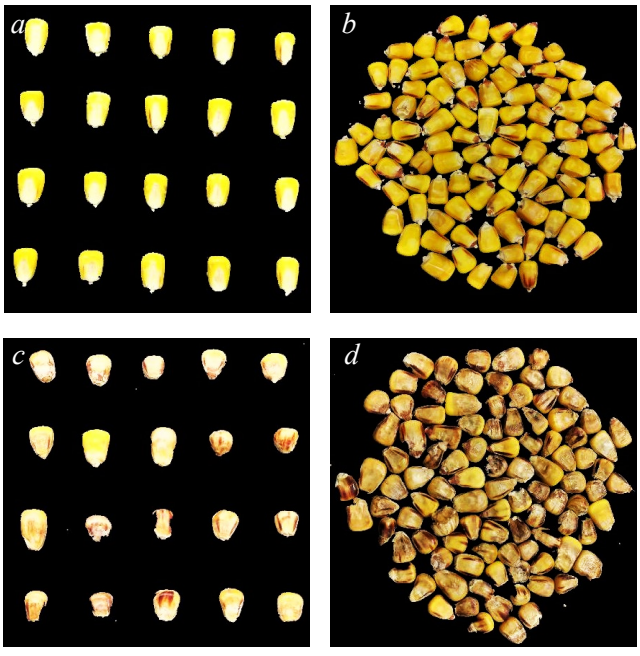

Fig 5. Segmented images from the graph cut method (a) Healthy - non touching (b) Healthy - touching (c) Fusarium infected - non touching (d) Fusarium infected – touching.

infected corn grains. However, this method could not capture the grain edges and corners accurately. In some grains, edges of the grains were considered as the background and in some other grains, background pixels were included in the ROI. This variability would have huge impacts in the classification model as edges of the grain is one of the most essential regions for extracting strong features. While this method had the advantage of extracting accurate information inside the corn grains including regions with colour variation in the endosperm and germ, it also had the disadvantage of time consumption and inter and intra-variations from person to person (Starmans et al. 2020).

Clustering segmentation The edges of the kernels were clearly segmented from the background (Fig. 3) because this method treats each corn kernel as a cluster and all pixels associated with that kernel were grouped into that cluster. Also, the variance within each cluster were minimum resulting in clear segmentation. However, some of the pixels from the ROI, especially from the bottom of the germ portion of the grains, which were dark coloured were treated as the background and was grouped as a background cluster. Although, the advantage of this technique is that it is very simple, highly efficient and could be utilized for large datasets, the disadvantage is that, since it is distance based, this algorithm follows no specific selection criteria and become difficult to estimate. Also, this method is only applicable to datasets which are convex (Pouladzadeh et al. 2014).

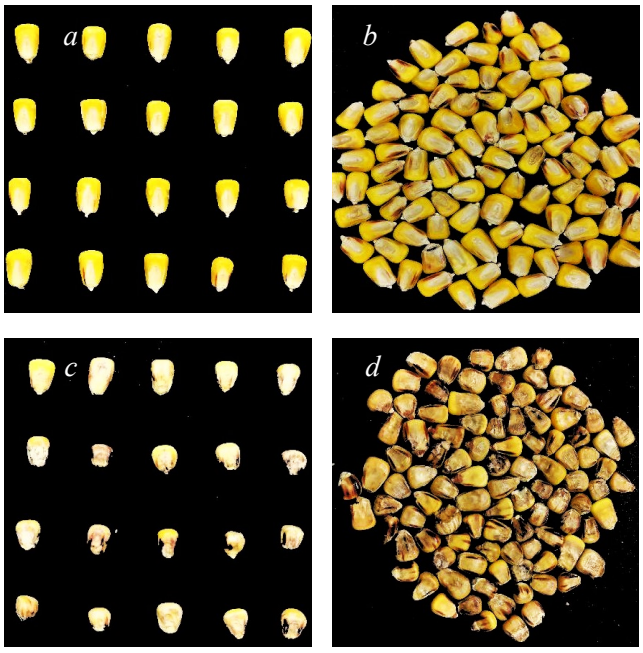

Fig 6. Segmented images from the colour thresholding method (a) Healthy - non touching (b) Healthy - touching (c) Fusarium infected - non touching (d) Fusarium infected – touching.

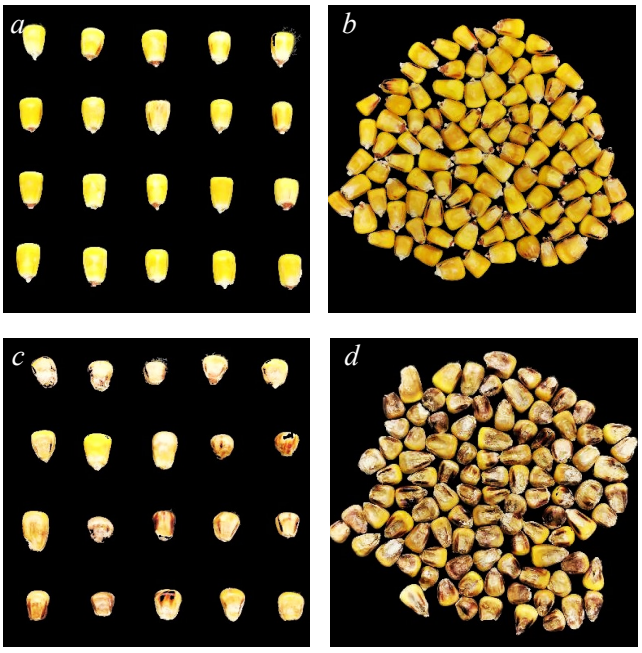

Fig 7. Segmented images from the watershed method (a) Healthy - non touching (b) Healthy - touching (c) Fusarium infected - non touching (d) Fusarium infected – touching.

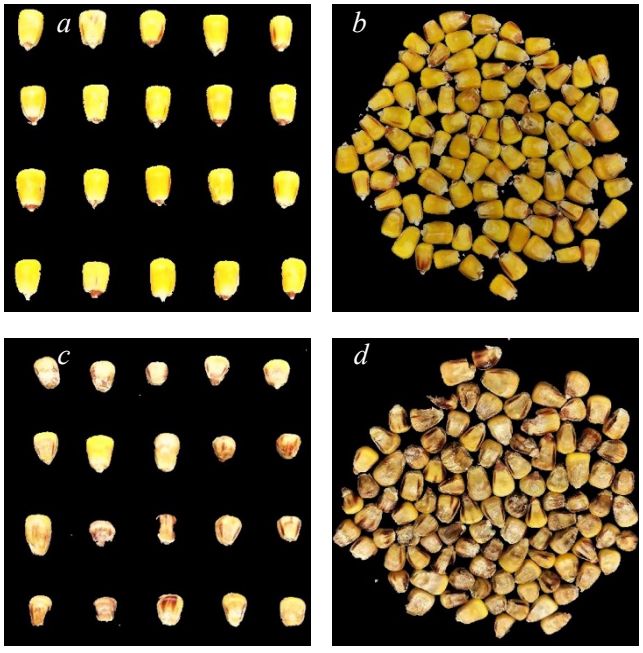

Fig 8. Segmented images from Otsu's thresholding method (a) Healthy - non touching (b) Healthy - touching (c) Fusarium infected - non touching (d) Fusarium infected – touching.

Flood Fill based object segmentation Flood fill or seed fill algorithm determines the ROI based on its connections with the given node. For healthy grains, the segmentation was accurate with very minimal variations in the darker regions on the grain surface, whereas for the infected corn grains, a lot of variations could be seen (Fig. 4). This was mainly due to the huge difference between the start node and the target node (Lee and Kang 2010). Since the infected kernels had a darker endosperm and germ regions, when the algorithm moves to these regions, it considers them as background pixels and does not change them to the replacement colour and instead it moves over to the next connected node. This could be observed in both the non-touching and touching corn grains. This resulted in loss of features from the grain surface.

Graph cut segmentation The graph cut algorithm segmented both the individual and touching corn kernels accurately. It clearly distinguished the background pixels in healthy kernels but showed some variations in detecting the edges of the infected kernels (Fig. 5), especially where the pixels coincide with the background thereby assigning higher weights to the background nodes. This was achieved because, it optimized the energy function over the segmentation. The background and foreground pixels were modelled using Gaussian distribution and used the intensities as seed pixels to get both the histograms. Although, some overlap was observed in the touching

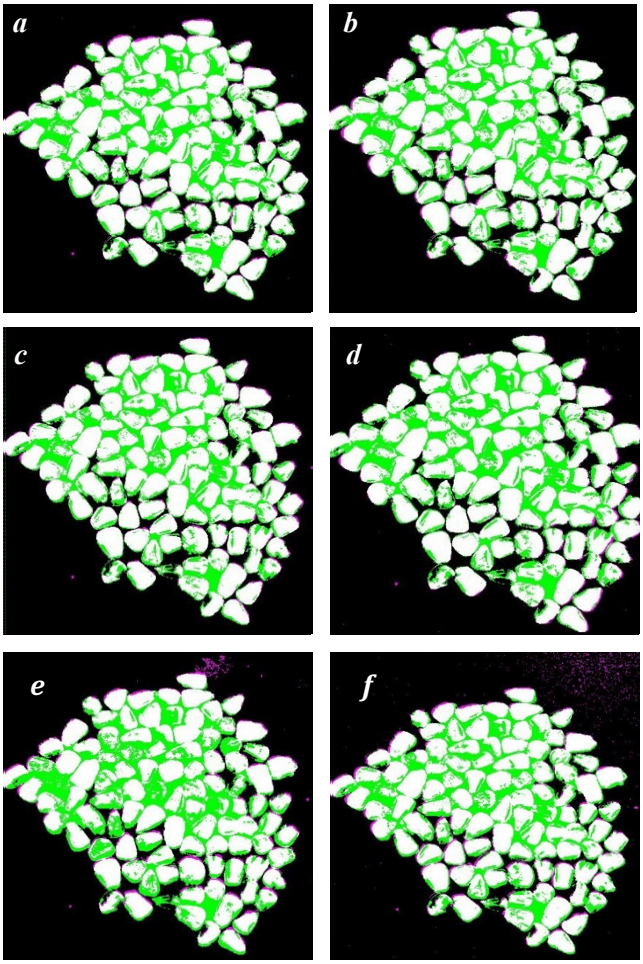

Fig 9. Sample images of healthy touching kernels (predicted mask overlapped on the gold standard) after evaluation of segmentation methods (a) Clustering (b)Flood fill (c) Graph cut (d) Colour thresholding (e) Watershed (f) Otsu's thresholding method.

kernels, this happened only where the background pixels were not clearly visible. Visually, graph cut appeared to be a suitable method for segmenting corn kernels.

Colour thresholding This technique segmented the healthy kernels clearly as there was a distinct colour variation between the grains and the background. The red channel (R) had a greater influence than the green and blue channel. Both the edges and the whole ROI of each grain were clearly segmented in the healthy grains by this technique (Fig 6). However, for the Fusarium infected grains, the edges were not clearly segmented because of the overlap in the RGB channels of foreground with that of the background. Widening the channels resulted in inclusion of background pixels whereas narrowing the channels resulted in exclusion of foreground pixels. Therefore, the optimal threshold was fixed for RGB channels with lesser background pixels and each of the images was segmented.

Watershed segmentation The watershed algorithm segmented the touching kernels in both healthy and infected datasets distinctly than the non-touching kernels (Fig.7). The background was not clearly marked in both the cases, but the foreground objects were more distinguishable in the touching kernels. This was because the algorithm identified the catchment basins and ridge lines in the image and treated it as a surface where light pixels were considered high and dark pixels were considered low. The major drawback of this method was the over-segmentation caused by excessive extreme values from the disturbances and noises in the image. This could be observed in the non-touching kernels where the disturbances in the background were interfering with the foreground objects.

Otsu's thresholding The Otsu's thresholding method detected the edges of the kernels, but failed to accurately identify the entire kernel surface, especially in case of infected kernels. Since there were dark patches on the infected kernels, the algorithm assigned those pixels to the background class. From Fig 8, it could be observed that some of the surface portions of the infected kernels had black patches which meant that they were considered as background and not segmented. In case of healthy kernels, the grain surface, edges and even the corn ear portion (the small part that will be attached to the whole corn ear) were segmented clearly.

Segmentation accuracy

The Jaccard and Dice coefficient evaluation metrics were calculated for all the images in the dataset for each of the segmentation methods. The average metric coefficient for each segmentation method is calculated and shown in Table 2 and 3.

Jaccard similarity index The segmentation methods had a significant effect ($p<0.05$) on the segmentation accuracy determined by Jaccard similarity index. Flood fill and graph cut methods showed the highest average segmentation accuracy of 77% and watershed segmentation showed the least segmentation accuracy of 59%. In the healthy grains, the segmentation accuracy was high for the touching kernels (78%) than the non-touching kernels (71%). In the *Fusarium* infected grains, the segmentation accuracy was 70% for both touching and non-touching kernels. Also, when comparing the effect of germ and endosperm portion of the grains, the segmentation accuracy was higher for the grains with germ side above (73%) than the grains with the endosperm side (71%).

Dice coefficient The segmentation methods had significant effect ($p<0.05$) on the accuracy of segmentation determined by Dice evaluation metrics. Flood fill and graph cut methods showed the highest average segmentation accuracy of 87% and watershed segmentation showed the least accuracy of 72%. In the healthy grains, segmentation accuracy was high for touching kernels (87.5%), whereas in the *Fusarium* infected grains, the segmentation accuracy was 81% for both touching and non-touching kernels. Even though watershed and Otsu's method had greater accuracy

Table 2: Jaccard Similarity evaluation metrics for each segmentation method (n=150).

Segmentation method	Healthy grains				Fusarium infected grains			
	Non-touching		Touching		Non-touching		Touching	
	Endosperm side	Germ side	Endosperm side	Germ side	Endosperm side	Germ side	Endosperm side	Germ side
Clustering	$0.78^{a*} \pm 0.009$	$0.81^{a} \pm 0.005$	$0.79^{a} \pm 0.013$	$0.74^{a} \pm 0.076$	$0.72^{a} \pm 0.063$	$0.87^{a} \pm 0.012$	$0.70^{a} \pm 0.014$	$0.67^{a} \pm 0.011$
Flood fill	$0.88^{b} \pm 0.023$	$0.78^{b} \pm 0.013$	$0.81^{b} \pm 0.015$	$0.76^{ab} \pm 0.024$	$0.71^{a} \pm 0.029$	$0.80^{b} \pm 0.031$	$0.70^{a} \pm 0.017$	$0.75^{b} \pm 0.019$
Graph cut	$0.90^{c} \pm 0.033$	$0.82^{c} \pm 0.014$	$0.77^{c} \pm 0.019$	$0.72^{ac} \pm 0.021$	$0.76^{b} \pm 0.022$	$0.78^{c} \pm 0.008$	$0.71^{b} \pm 0.007$	$0.69^{c} \pm 0.021$
Colour thresholding	$0.76^{a} \pm 0.085$	$0.86^{d} \pm 0.022$	$0.79^{a,d} \pm 0.015$	$0.81^{d} \pm 0.046$	$0.70^{a} \pm 0.062$	$0.80^{b} \pm 0.029$	$0.70^{a} \pm 0.018$	$0.67^{a} \pm 0.029$
Watershed	$0.46^{d} \pm 0.028$	$0.47^{e} \pm 0.032$	$0.74^{e} \pm 0.038$	$0.77^{e} \pm 0.017$	$0.42^{c} \pm 0.019$	$0.48^{d} \pm 0.026$	$0.64^{c} \pm 0.027$	$0.73^{d} \pm 0.038$
Otsu's thresholding	$0.46^{d} \pm 0.027$	$0.50^{f} \pm 0.041$	$0.80^{abd} \pm 0.039$	$0.82^{d} \pm 0.032$	$0.65^{d} \pm 0.018$	$0.67^{e} \pm 0.028$	$0.67^{d} \pm 0.022$	$0.72^{d} \pm 0.035$

*Values with same letters in a column are not significantly different (α=0.05)

Table 3: Dice coefficient evaluation metrics for each segmentation method (n=150).

Segmentation method	Healthy grains				Fusarium infected grains			
	Non-touching		Touching		Non-touching		Touching	
	Endosperm side	Germ side	Endosperm side	Germ side	Endosperm side	Germ side	Endosperm side	Germ side
Clustering	$0.88^{a*} \pm 0.015$	$0.89^{a} \pm 0.023$	$0.88^{a} \pm 0.008$	$0.85^{a} \pm 0.022$	$0.83^{a} \pm 0.016$	$0.93^{a} \pm 0.009$	$0.82^{a} \pm 0.029$	$0.80^{a} \pm 0.018$
Flood fill	$0.94^{b} \pm 0.023$	$0.88^{a} \pm 0.036$	$0.89^{b} \pm 0.017$	$0.86^{ab} \pm 0.034$	$0.83^{a} \pm 0.028$	$0.89^{b} \pm 0.019$	$0.83^{a} \pm 0.024$	$0.86^{b} \pm 0.032$
Graph cut	$0.95^{b} \pm 0.025$	$0.90^{b} \pm 0.017$	$0.87^{c} \pm 0.015$	$0.84^{a} \pm 0.023$	$0.86^{b} \pm 0.019$	$0.88^{c} \pm 0.021$	$0.83^{a} \pm 0.016$	$0.81^{c} \pm 0.004$
Colour thresholding	$0.86^{c} \pm 0.027$	$0.93^{c} \pm 0.019$	$0.88^{abc} \pm 0.028$	$0.90^{c} \pm 0.034$	$0.83^{a} \pm 0.087$	$0.89^{bc} \pm 0.031$	$0.82^{a} \pm 0.022$	$0.80^{a} \pm 0.018$
Watershed	$0.63^{d} \pm 0.038$	$0.64^{d} \pm 0.031$	$0.85^{d} \pm 0.027$	$0.87^{b} \pm 0.041$	$0.59^{c} \pm 0.028$	$0.55^{d} \pm 0.025$	$0.78^{b} \pm 0.029$	$0.85^{bd} \pm 0.033$
Otsu's thresholding	$0.63^{d} \pm 0.022$	$0.67^{e} \pm 0.024$	$0.89^{b} \pm 0.017$	$0.90^{c} \pm 0.007$	$0.79^{d} \pm 0.029$	$0.79^{e} \pm 0.034$	$0.80^{c} \pm 0.042$	$0.84^{d} \pm 0.028$

*Values with same letters in a column are not significantly different (α=0.05)

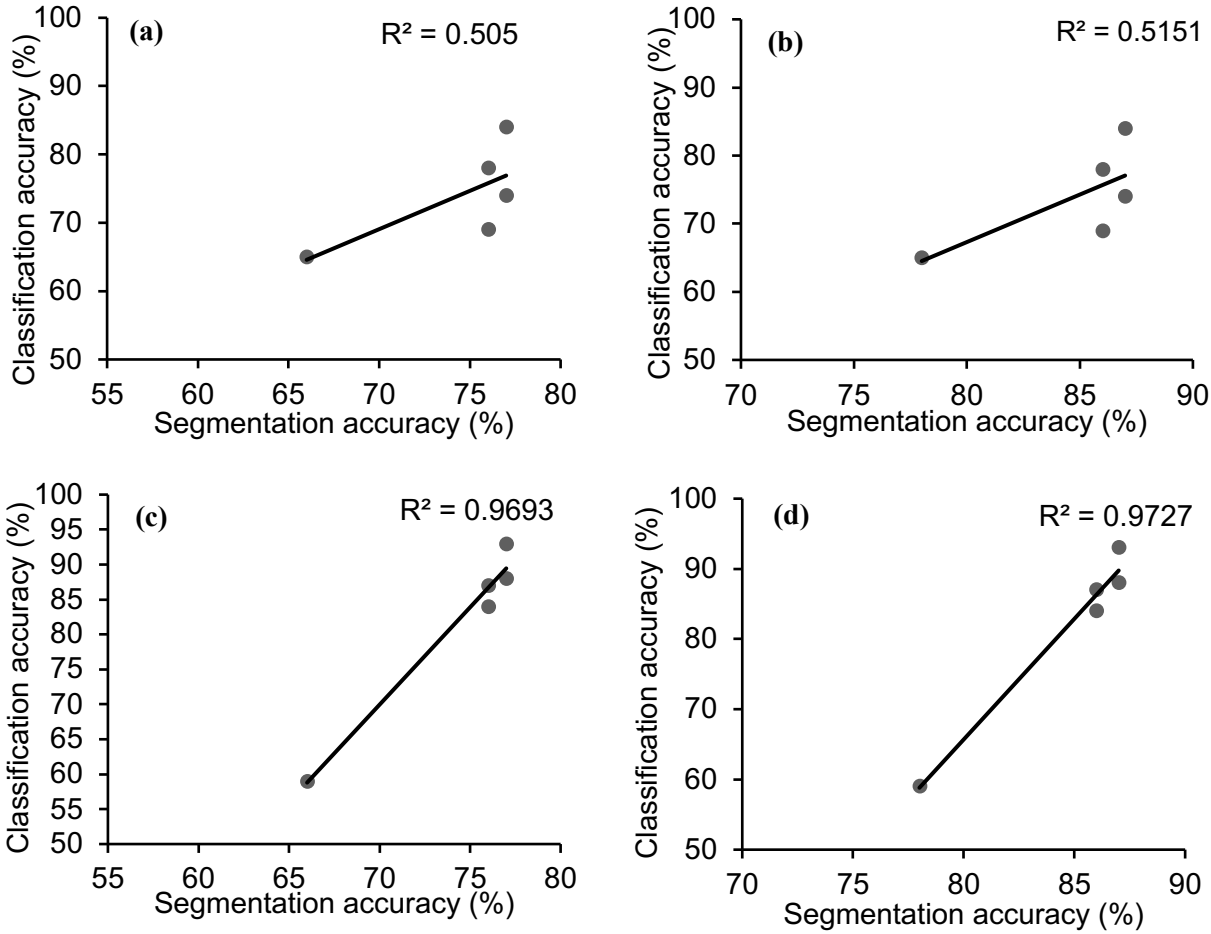

Fig 10. Effect of segmentation accuracy on classification accuracy (a) Jaccard similarity index vs SVM (b) Dice coefficient vs SVM (c) Jaccard similarity index vs Pretrained CNN (d) Dice coefficient vs Pretrained CNN.

for touching kernels, they did not perform well for non-touching kernels resulting in a lower average segmentation accuracy. This could be observed in the segmentation masks overlapped on the gold standard mask given in Fig 9. In the first four segmentation methods, variations could only be seen in the spaces between the touching kernels, whereas in watershed and Otsu method, it considered some of the background pixels as the foreground ROI which further decreased the segmentation accuracy.

Classification models

Support vector machine model In each segmentation method nine colour features and thirteen geometric features were extracted from the segmented regions of each image and an SVM based multiclass classifier model was developed (training:validation - 60%:40%) with two classes - Healthy and *Fusarium* infected. The overall accuracy of each segmentation method is shown in Table 4. All segmentation methods except Otsu's and colour thresholding showed an accuracy greater than 70%. Graph cut method showed the highest accuracy of 84% followed by gold standard method with 82%. Although false negatives could be seen, there were very minimal false positives. This indicated that the number of *Fusarium* infected corn grains wrongly classified as healthy were minimal.

Pretrained CNN model: Based on the classification output, a confusion matrix was plotted, and the overall classification accuracy was calculated for each segmentation method as observed in Table 4. The segmentation methods showed an increase in the accuracy of the pretrained CNN model. Flood fill showed the highest accuracy of 93% followed by graph cut and colour thresholding with 88% and 87%, respectively. Overall, it could be seen that flood fill, graph cut, and colour thresholding are the top three segmentation methods that are more suitable for pretrained neural networks to efficiently classify both healthy and *Fusarium* infected corn grains. The results further support the findings of Pouladzadeh (2014) where the implementation of graph-cut segmentation algorithm for food classification and recognition and showed a 15% increase in food classification accuracy.

Table 4. Classification accuracies for each segmentation method.

Segmentation method	Classification accuracy	
	Support vector	Pre-trained CNN
No segmentation	-	73
Gold Standard	82	85
Clustering	78	84
Flood Fill	74	93
Graph cut	84	88
Colour thresholding	69	87
Watershed	79	61
Otsu's thresholding	65	59

Effect of segmentation accuracy on classification accuracy

The correlation between the segmentation accuracy (Jaccard similarity index and Dice coefficient metrics) and classification accuracy (SVM and pretrained CNN) is shown in Fig. 10. Overall, it could be observed that the segmentation accuracy has a positive correlation with classification accuracy. A strong positive correlation was observed between segmentation accuracy and pretrained CNN classification accuracy with coefficient of determination (R^2) values of 0.9693 and 0.9727 for Jaccard and Dice evaluation metrics, respectively. However, the correlation was moderately positive between segmentation accuracy and SVM classification accuracy with the R^2 values ranging from 0.505 for Jaccard and 0.5151 for Dice evaluation metrics. The results showed that proper segmentation with higher segmentation accuracy is leading to improved classification, further supporting the literarure (Gao et al. 2007).

CONCLUSIONS

Graph cut showed the highest classification accuracy (84%) for the developed SVM based machine learning classification model in discriminating the healthy and *Fusarium* infected corn grains. Most of the segmentation methods clearly identified and segmented the healthy kernels but did not deliver the same performance for *Fusarium* infected kernels. This was mainly due to the large colour variations in the infected grains, most of which were wrongly segmented as the background pixels. Also, the segmentation methods showed higher segmentation accuracies for the touching grains rather than the non-touching grains. In case of pretrained CNN model, flood fill method showed the highest classification accuracy of 93% followed by graph cut (88%) and colour thresholding (87%). Watershed and Otsu's thresholding method showed higher classification accuracies for touching kernels but failed to segment the non-touching kernels accurately. A high correlation was also observed between segmentation accuracy and classification accuracy, especially with the pretrained CNN model with R^2 values of 0.9693(Jaccard similarity index) and 0.9727 (Dice coefficient). For further research, individual grain testing could be performed so that the model can efficiently identify infected grains when healthy and infected grains are mixed together. The appropriate segmentation methods could be optimized and incorporated in developing a machinery that could be installed in the farms and corn processing industries that accurately discriminates the healthy and infected kernels. The results strongly suggests that for future research on image-based applications, investigation on various segmentation techniques would provide us with the suitable method that would contribute to the most efficient classification model development with optimized accuracy.

ACKNOWLEDGEMENT

The authors would like to acknowledge the Barrett Family Foundation, and Natural Sciences and Engineering Research Council of Canada (NSERC) for financial support, and Ontario Ministry of Agriculture, Food and Rural Affairs (OMAFRA) for providing the corn grain samples.

REFERENCES

Agelet, Lidia Esteve, David D. Ellis, Susan Duvick, A. Susana Goggi, Charles R. Hurburgh, and Candice A. Gardner, 2012. Feasibility of near infrared spectroscopy for analyzing corn kernel damage and viability of soybean and corn kernels. *Journal of Cereal Science* 55(2): 160-165. https://doi.org/10.1016/j.jcs.2011.11.002

Belaid, L.J. and Mourou, W., 2009. Image segmentation: a watershed transformation algorithm. *Image Analysis & Stereology* 28(2):93-102. https://doi.org/10.5566/ias.v28.p93-102

Bieniek, A. and Moga, A., 2000. An efficient watershed algorithm based on connected components. *Pattern recognition* 33(6):907-916. https://doi.org/10.1016/S0031-3203(99)00154-5

Del Fiore, A., M. Reverberi, A. Ricelli, F. Pinzari, S. Serranti, A. A. Fabbri, G. Bonifazi, and C. Fanelli, 2010. Early detection of toxigenic fungi on maize by hyperspectral imaging analysis. *International journal of food microbiology* 144(1):64-71. https://doi.org/10.1016/j.ijfoodmicro.2010.08.001

Dhanachandra, N. and Chanu, Y.J., 2017. A survey on image segmentation methods using clustering techniques. *European Journal of Engineering Research and Science* 2(1):15-20. https://doi.org/10.24018/ejeng.2017.2.1.237

DON testing protocols, 2019. Ontario Grain Farmer Magazine, Grain Farmers of Ontario, https://ontariograinfarmer.ca/2019/09/01/don-testing-protocols/

Gao, Y., N. Kerle, J.F. Mas, Navarrete and I. Niemeyer. 2007. Optimized image segmentation and its effect on classification accuracy. In *Poster Session on 5th international Symposium on Spatial Data Quality, Enschede, The Netherlands*.

Kulkarni, N., 2012. Colour thresholding method for image segmentation of natural images. International Journal of

Image, *Graphics and Signal Processing* 4(1):28. https://doi.org/10.5815/ijigsp.2012.01.04

Kushiro, M., 2008. Effects of milling and cooking processes on the deoxynivalenol content in wheat. *International journal of molecular sciences* 9(11):2127-2145. https://doi.org/10.3390/ijms9112127

Lee, J. and Kang, H., 2010. Flood fill mean shift: A robust segmentation algorithm. *International Journal of Control, Automation and Systems* 8(6):1313-1319. https://doi.org/10.1007/s12555-010-0617-6

Longzhe, Q., 2011. Automatic Segmentation Method of Touching Corn Kernels in Digital Image Based on Improved Watershed Algorithm. 2011 Int. Conf. New Technol. Agric. 34-37. https://doi.org/10.1109/ICAE.2011.5943743

McAllister, P., Zheng, H., Bond, R. and Moorhead, A., 2018. Combining deep residual neural network features with supervised machine learning algorithms to classify diverse food image datasets. *Computers in biology and medicine* 95:217-233. https://doi.org/10.1016/j.compbiomed.2018.02.008

Pal, N.R. and Pal, S.K., 1993. A review on image segmentation techniques. *Pattern recognition* 26(9):1277-1294. https://doi.org/10.1016/0031-3203(93)90135-J

Panigrahi, S., Bern, C.J., Marley, S.J., 1995. Background Segmentation and Dimensional Measurement of Corn Germplasm Background Segmentation and Dimensional Measurement of Corn. https://doi.org/10.13031/2013.27841

Shi, R., Ngan, K.N. and Li, S., 2014, October. Jaccard index compensation for object segmentation evaluation. In 2014 IEEE International Conference on Image Processing (ICIP) (pp. 4457-4461). IEEE. https://doi.org/10.1109/ICIP.2014.7025904

Pestka, J.J., 2010. Deoxynivalenol: mechanisms of action, human exposure, and toxicological relevance. *Archives of toxicology* 84(9):663-679. https://doi.org/10.1007/s00204-010-0579-8

Pouladzadeh, P., Shirmohammadi, S. and Yassine, A., 2014, June. Using graph cut segmentation for food calorie measurement. In 2014 IEEE International Symposium on Medical Measurements and Applications (MeMeA) (pp. 1-6). IEEE. https://doi.org/10.1109/MeMeA.2014.6860137

Ran, R., Wang, C., Han, Z., Wu, A., Zhang, D. and Shi, J., 2013. Determination of deoxynivalenol (DON) and its derivatives: Current status of analytical methods. *Food Control* 34(1):138-148. https://doi.org/10.1016/j.foodcont.2013.04.026

Rathna Priya, T.R. and Manickavasagan, A., 2021. Characterising corn grain using infrared imaging and spectroscopic techniques: a review. *Journal of Food Measurement and Characterization*. 15:3234-3249.

Senthilkumaran, N. and Vaithegi, S., 2016. Image segmentation by using thresholding techniques for medical images. *Computer Science & Engineering: An International Journal* 6(1):1-13. https://doi.org/10.5121/cseij.2016.6101

Serna-Saldivar, S.O. and Carrillo, E.P., 2019. Food uses of whole corn and dry-milled fractions. In Corn (pp. 435-467). AACC International Press. https://doi.org/10.1016/B978-0-12-811971-6.00016-4

Sha, C., Hou, J. and Cui, H., 2016. A robust 2D Otsu's thresholding method in image segmentation. *Journal of Visual Communication and Image Representation* 41:339-351. https://doi.org/10.1016/j.jvcir.2016.10.013

Skourt, B.A., El Hassani, A. and Majda, A., 2018. Lung CT image segmentation using deep neural networks. *Procedia Computer Science* 127:109-113. https://doi.org/10.1016/j.procs.2018.01.104

Starmans, M.P., van der Voort, S.R., Tovar, J.M.C., Veenland, J.F., Klein, S. and Niessen, W.J., 2020. Radiomics: data mining using quantitative medical image features. In Handbook of Medical Image Computing and Computer Assisted Intervention (pp. 429-456). Academic Press. https://doi.org/10.1016/B978-0-12-816176-0.00023-5

Statistics Canada, 2020. Production of principal field crops. https://www150.statcan.gc.ca/n1/daily-quotidien/201203/dq201203b-eng.htm

Veksler, O., 2008, October. Star shape prior for graph-cut image segmentation. In European Conference on Computer Vision (pp. 454-467). Springer, Berlin, Heidelberg. https://doi.org/10.1007/978-3-540-88690-7_34

Yuheng, S. and Hao, Y., 2017. Image segmentation algorithms overview. arXiv preprint arXiv:1707.02051.